Power Take-Off Design Study for a Small-Scale Oscillating Surge Wave Energy Converter for Powering the Blue Economy Applications

Preprint

Jackson Wills,[1] Nathan Tom,[2] and Senu Sirnivas[2]

1 University of Minnesota
2 National Renewable Energy Laboratory

Presented at ASME 2023 International Mechanical Engineering Congress and Exposition (IMECE2023)
New Orleans, Louisiana
October 29–November 2, 2023

NREL is a national laboratory of the U.S. Department of Energy
Office of Energy Efficiency & Renewable Energy
Operated by the Alliance for Sustainable Energy, LLC

This report is available at no cost from the National Renewable Energy Laboratory (NREL) at www.nrel.gov/publications.

Contract No. DE-AC36-08GO28308

Conference Paper
NREL/CP-5700-86187
November 2023

Power Take-Off Design Study for a Small-Scale Oscillating Surge Wave Energy Converter for Powering the Blue Economy Applications

Preprint

Jackson Wills,[1] Nathan Tom,[2] and Senu Sirnivas[2]

1 University of Minnesota
2 National Renewable Energy Laboratory

Suggested Citation
Wills, Jackson, Nathan Tom, and Senu Sirnivas. 2023. *Power Take-Off Design Study for a Small-Scale Oscillating Surge Wave Energy Converter for Powering the Blue Economy Applications: Preprint*. Golden, CO: National Renewable Energy Laboratory. NREL/CP-5700-86187. https://www.nrel.gov/docs/fy24osti/86187.pdf.

Conference Paper
NREL/CP-5700-86187
November 2023

National Renewable Energy Laboratory
15013 Denver West Parkway
Golden, CO 80401
303-275-3000 • www.nrel.gov

NOTICE

This work was authored in part by the National Renewable Energy Laboratory, operated by Alliance for Sustainable Energy, LLC, for the U.S. Department of Energy (DOE) under Contract No. DE-AC36-08GO28308. Funding provided by U.S. Department of Energy Office of Energy Efficiency and Renewable Energy Water Power Technologies Office. The views expressed herein do not necessarily represent the views of the DOE or the U.S. Government. The U.S. Government retains and the publisher, by accepting the article for publication, acknowledges that the U.S. Government retains a nonexclusive, paid-up, irrevocable, worldwide license to publish or reproduce the published form of this work, or allow others to do so, for U.S. Government purposes.

Cover Photos by Dennis Schroeder: (clockwise, left to right) NREL 51934, NREL 45897, NREL 42160, NREL 45891, NREL 48097, NREL 46526.

POWER TAKE-OFF DESIGN STUDY FOR A SMALL-SCALE OSCILLATING SURGE WAVE ENERGY CONVERTER FOR POWERING THE BLUE ECONOMY APPLICATIONS

Jackson Wills[1], Nathan Tom[2,*], Senu Sirnivas[2]

[1]University of Minnesota, Minneapolis, MN
[2]National Renewable Energy Laboratory, Golden, CO

ABSTRACT

The power take-off (PTO) is an integral part of wave energy conversion, and the design process is nontrivial. Better PTOs, and better processes for selecting and designing PTO architectures for various applications, would benefit devices that assist in powering the blue economy by decreasing time and money spent on PTO design and increasing the overall energy capture performance of these devices. This paper chronicles the selection process of a PTO for a small-scale surge-type wave energy converter (WEC) for the purpose of informing future PTO selection processes. Three PTO architectures are evaluated in WEC-Sim: a hydraulic check valve PTO, a hydraulic active valving PTO, and a directly electrified PTO. Simple models of each PTO are constructed. Because a model for the small-scale device was initially unavailable, the PTOs are simulated on a large-scale device. The results are scaled down using Froude scaling and compared to results from directly simulating a small-scale model. Strong assumptions are made because this work is early in the design stages, and a coarse look at PTO options was desired. Specifically, the effectiveness of controls is investigated, along with the efficiency of energy conversion. However, energy capture is only part of the consideration; there are also logistic concerns to be considered when selecting a PTO. For example, components for large-scale WECs are so large and expensive that it may make sense to custom-build PTO components, but small-scale WECs would benefit from off-the-shelf availability because the cost of customization would be a significant portion of the total capital cost of deployment at a small scale. Submersible, off-the-shelf components are much easier to source for hydraulic PTOs. Because of highly effective controls, efficient energy conversion, and availability of marine-grade components, an active valving hydraulic PTO is selected for this small-scale surge-type WEC.

Keywords: Energy Conversion/Systems, Renewable Energy, Modeling and Simulation

*Corresponding author: nathan.tom@nrel.gov

1. INTRODUCTION

The power take-off (PTO) is the system in place between the mechanical energy present in the motion of the wave energy converter (WEC) and the useful product, such as electricity or desalinated water. PTOs are also used in other machines, like tractors, to converts the chemical energy of gasoline into the desired mechanical work the machine was made to produce. However, the PTO is not only responsible for converting different forms of energy; it is also the means by which the device can be controlled. As this analysis shows, the control scheme has a large effect on the amount of output produced by a WEC (electricity or fresh water, though the focus of this work is on electricity). Designing PTOs for wave energy applications is especially difficult, but improving these systems will benefit the wave energy industry. The first and most obvious challenge is the marine environment. The components of the PTO must be able to sustain not only days of long, intense storms but also the day-to-day wear from the saline environment [1]. The next challenge is the manner in which the waves transmit energy. Large fluctuations in power are present, both in the time span of seconds as each wave reaches the device, and in the time span of hours and days as the weather changes the sea state [2]. The goal is to create a device that is useful, with output that is worth the cost.

The desired characteristics of a PTO are 1) to be robust and durable for the marine environment, 2) to have low-cost components, and 3) to have high useful product output. A high-output product is achieved through effective control strategies and highly efficient power conversion chains. In search of these characteristics, we simulated three PTOs using our own models for the PTOs, and WEC-Sim for the WEC dynamics [3]. Because of the availability of the standard oscillating surge wave energy converter (OSWEC) WEC-Sim model (WEC-Sim comes with an OSWEC example folder), this WEC was used to compare each PTO. The PTOs considered are 1) a check valve PTO, 2) an active valving PTO, and 3) a directly electrified PTO. Models were constructed for each PTO. The constructed PTOs models

FIGURE 1: THE HAWAI'I WAVE SURGE ENERGY CONVERTER (HAWSEC). THE BROAD FACE OF THE FLAP IS ROUGHLY 1 × 1 M.

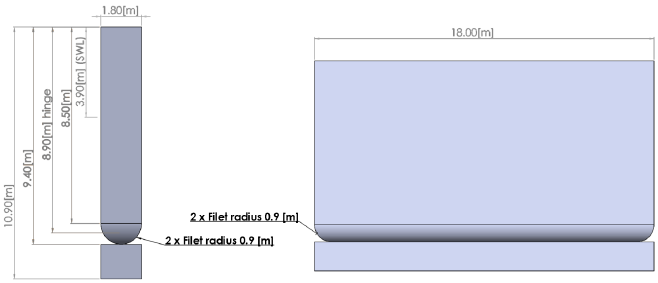

FIGURE 2: THE STANDARD WEC-SIM OSWEC MODEL IS A FIXED-BOTTOM OSWEC THAT IS SIMILAR TO THE HAWSEC IN FORM BUT NOT IN SIZE [3].

are simpler and lower fidelity than Simscape Fluids or PTO-Sim models. Simple models were used as a starting point because of the lower number of parameters and lower computational cost. Each PTO model calculates a torque that is directly applied to the Simscape revolute joint corresponding to the axis of rotation of the flap in the WEC-Sim Simulink file. The PTOs were compared with respect to how well each of the desired characteristics was achieved.

The goal of this work was to design a PTO for a small-scale WEC designed at the University of Hawai'i, called the Hawai'i Wave Surge Energy Converter (HAWSEC). The standard OSWEC is similar to the HAWSEC model, but it is much larger (see Figures 1 and 2). The standard OSWEC was simulated as a proxy because the HAWSEC model was originally unavailable. The results were scaled down to the HAWSEC using Froude scaling, which attempts to scale gravitational and inertial effects evenly. Finally, the HAWSEC was simulated at scale, and the results were compared to the scaled standard OSWEC results.

Section 2 discusses the PTOs and the models used to simulate them. Section 3 shows the frequency response of the device as well as the control scheme used for this study. Section 4 shows the results for each PTO and the effectiveness of scaling between the standard OSWEC and HAWSEC models. Study limitations are discussed in Section 5. Finally, the overall results are discussed along with practical concerns in Section 6.

2. POWER TAKE-OFFS

Three PTOs from literature were selected to be analyzed. They were selected because of their widespread use and/or demonstrated potential. Models were made for each PTO and each was simulated under idealized conditions, but care was taken to ensure that each PTO was given roughly equally stringent assumptions.

2.1 Check Valve PTO

The check valve PTO is one of most highly cited and studied hydraulic PTOs [4–6]. A schematic of this PTO is shown in Figure 3. As the flap moves, the cylinder is extended and retracted. The system of check valves (also called rectifying valves) ensures that high-pressure fluid is always on the side of the piston that opposes motion. This design serves two main functions: 1) it enacts a Coulomb damping control force on the device and 2) it pumps fluid from the fluid reservoir to the high-pressure accumulator. Usually, the check valve PTO is shown with two accumulators, one at high pressure and the other at low pressure. While using a low pressure accumulator does reduce the potential for cavitation, an elevated reservoir is used here because it is cheaper and easier to refill. Cavitation can only be prevented by locating the reservoir sufficiently close to the device. In this study, the reservoir was assumed to be close enough to the device such that the only significant pressure drop was through the valve; it was found that the speeds of the hydraulic cylinder were not large enough to cavitate the fluid as it passed through the valve.

The valves are assumed to actuate instantaneously, and the fluid is assumed to be incompressible. The PTO force enacted by this architecture is thus given by

$$F_{PTO} = \begin{cases} P_l A_c - P_h A_r & v \geq 0 \\ P_h A_c - P_l A_r & v < 0 \end{cases}$$

where P_h and P_l are the high and low system pressures, and A_c and A_r are the cap and rod side effective areas, respectively. The cylinder velocity is given by v, where positive velocity is extension.

Once fluid has been pumped into the high-pressure accumulator, the energy can be extracted using a hydraulic motor coupled to an electric generator. A control scheme is needed for the operation of this motor. The controller should ensure that the pressure of the accumulator stays in some desired range. In lieu of such a controller, the system is simulated using a relief valve in place of the motor and generator (see Figure 4). A relief valve is closed until the pressure across it reaches its set value, at which point it opens and allows flow from the accumulator to the tank.

In this study the check valve PTO was simulated as if a relief valve were used. The energy throttled by the relief valve was recorded, and the electricity output was estimated as if the motor and generator were used. This was done simply by assuming that the motor and generator constantly absorb mean power at 80% combined efficiency. This efficiency number was estimated and is

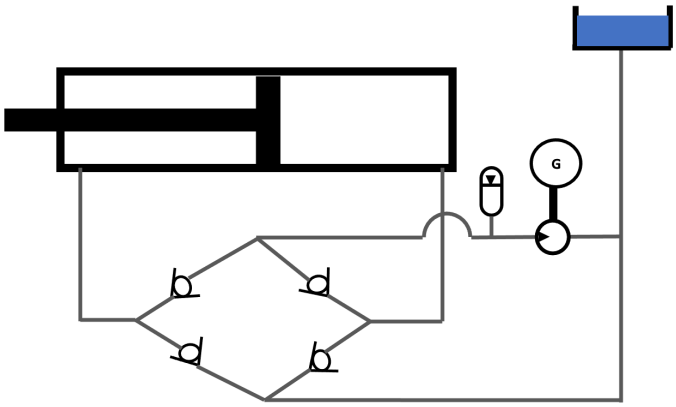

FIGURE 3: A SCHEMATIC OF THE CHECK VALVE POWER TAKE-OFF. THE CIRCUIT INCLUDES AN ELECTRIC GENERATOR COUPLED TO A HYDRAULIC MOTOR, WHICH DELIVERS FLOW FROM A HIGH PRESSURE ACCUMULATOR TO AN ELEVATED RESERVOIR OF HYDRAULIC OIL. A SERIES OF CHECK VALVES RECTIFY THE FLOW FROM THE HYDRAULIC CYLINDER SO THAT MOTION IN EITHER DIRECTION RESULTS IN FLOW TO THE ACCUMULATOR.

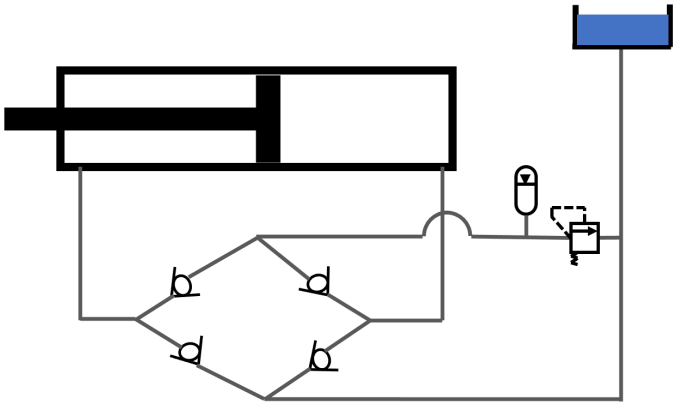

FIGURE 4: A SCHEMATIC OF THE SIMPLIFIED CHECK VALVE POWER TAKE-OFF WHERE A RELIEF VALVE REPLACES THE MOTOR GENERATOR COMBINATION.

probably overly optimistic. The loading on the components was fairly stable because of the hydraulic accumulation; therefore, a small range of operating conditions was used throughout the majority of operation. The components can be chosen such that this small operating region is near the peak efficiency region of the components, meaning that the electric generator and the hydraulic motor operate near 90% efficiency each, resulting in a net 80% for the two components together.

The gas in the accumulator was modeled as an isentropic process (PV^γ is constant: where P is pressure, V is volume, and γ is the heat capacity ratio). The model also assumed that the process of expanding and contracting the gas occurs without heat transfer (adiabatic), which results in a heat capacity ratio of 1.4. However, to simplify the analysis, the accumulator was made to be very large (300 m^3) such that there was little pressure change. Determining the size of the accumulator is not trivial and depends on the control strategy of the motor and the width of the acceptable accumulator pressure deviation. It was desired that the accumulator sizing be done after the PTO was selected.

The pressure of the accumulator was set to 4123 psi, because that was used in a similar device with an identical PTO [5]. The valves were assumed to have infinite bandwidth—that is, they open and close instantaneously. Pressure drop across the valves was modeled by the orifice equation, $Q = k\sqrt{\Delta P}$, where k is a constant for the valve. The value of k was chosen so that the pressure drop across the valve at max flow was about 10% of the system pressure (412.3 psi). The cap diameter of the hydraulic cylinder was set to 19 cm and the rod diameter was set to 12 cm.

2.2 Active Valving PTO

The active valving PTO has been previously proposed for three and four pressure rails [7] and is similar to a PTO designed for the Wavestar WEC in Denmark [8] as well as a PTO designed for the Pelamis WEC in Scotland [9]. A schematic of the PTO is shown in Figure 5. In this analysis, only two pressure rails are considered: high pressure and tank. Only considering two pressure rails makes this PTO similar to the check valve PTO, except the valves can be electrically controlled, which allows for more advanced control than the simple Coulomb damping control the check valves enact.

The modeling of this PTO is identical to the modeling of the check valve case, other than the operation of the valves. With two pressure rails and an uneven cylinder area ratio, there are four possible discrete PTO forces available. A continuous control force is calculated from a proportional-integral (PI) controller (discussed in Section 3). Of the four possible discrete forces, the closest force to the calculated PI control force is selected. The control of this PTO is further discussed in section 3.

The same parameter values were used in the active valving PTO as the check valve PTO.

2.3 Direct Electrification

Directly electrifying the PTO is a common approach in the literature [10, 11]. A surge-type WEC, like the HAWSEC, can be directly electrified by coupling an electric motor generator directly to the WEC at the axis of rotation, as shown in Figure 6. The angular speed of surge-type WECs is typically small and the torque is large. Electric generators typically require larger speeds and smaller torques, so gearing is needed. For simplicity, the gearing and electric motor generator are assumed to have a combined constant efficiency of 80%.

3. DYNAMICS AND CONTROL

A nonparametric system identification was performed on the standard OSWEC by applying a white noise input (torque input for the electric PTO, and force input for the hydraulic PTO) and measuring speed (rotational speed for the electric PTO and translational speed of the piston for the hydraulic PTO) [12]. The frequency response estimate for the WEC dynamics is shown in Figure 7. The system is essentially second-order at low frequencies but has some higher-order effects at high frequency. The nonparametric system response estimate gets progressively smoother as the frequency increases because many more high

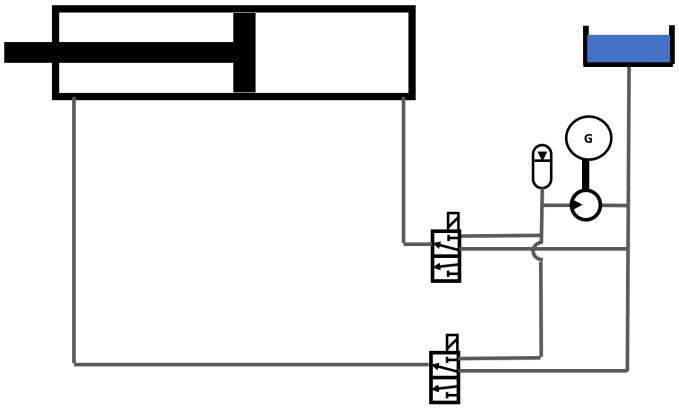

(a) Active valving PTO with two pressure rails

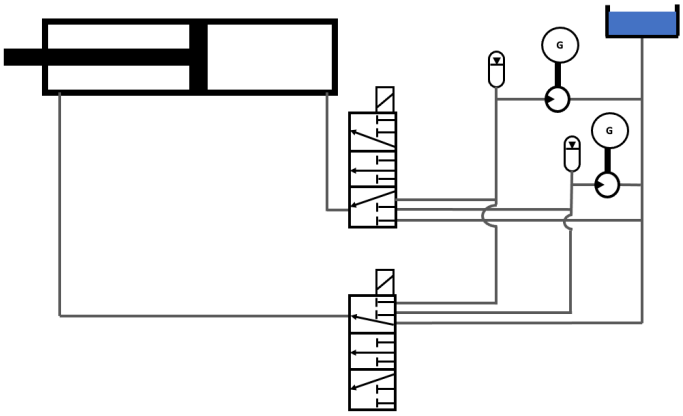

(b) Active valving PTO with three pressure rails

FIGURE 5: THE ACTIVE VALVING PTO ARCHITECTURES. SEPARATE GENERATORS ARE NOT REQUIRED FOR EACH RAIL BUT ARE DEPICTED THAT WAY FOR CLARITY. ONE GENERATOR COULD BE USED WITH MULTIPLE PRESSURE RAILS IF SOME VALVING SCHEME IS DEVELOPED.

frequency oscillations occur in a given amount of time than low frequency oscillations Estimates at high frequency have more available data than estimates at lower frequencies.

A simple complex conjugate controller (CCC) is used here [13]. The optimality of CCC can be proven using the maximum power transfer theorem for electric circuits. The WEC system dynamics can be written in terms of transfer functions:

$$\frac{F}{V} = Z_w \tag{1}$$

where Z_w is the impedance of the WEC and is complex valued, F is the force on the WEC and is given by $F = F_{exc} - F_{pto}$ where F_{exc} is the excitation force and F_{pto} is the PTO force, and V is the WEC rotational velocity.

These linear dynamics can be expressed as the equivalent electrical circuit shown in Figure 8. Velocity is the electrical analog to current, as it is the flow variable. Likewise, force is the effort variable and is analogous to voltage. In this manner, an electric circuit can be formulated that models the WEC dynamics identically as before.

The goal is to find the transfer function for the controller Z_p

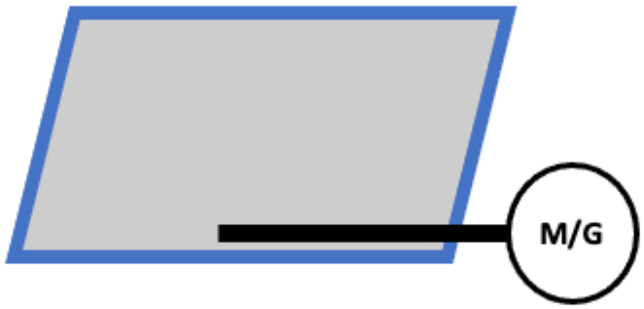

FIGURE 6: A DIRECTLY ELECTRIFIED PTO ARCHITECTURE FOR A SURGE-TYPE WEC. THE BLUE PARALLELOGRAM IS THE FLAP OF THE OSWEC. ATTACHED TO THE AXIS OF ROTATION OF THE FLAP IS AN ELECTRIC MOTOR GENERATOR, WHICH PROVIDES TORQUE TO THE DEVICE.

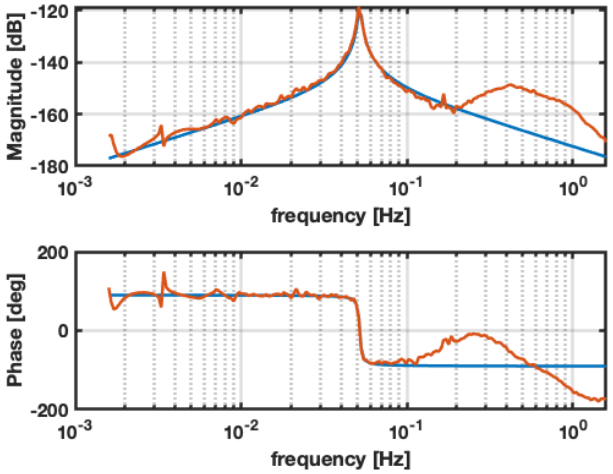

FIGURE 7: ESTIMATE OF SYSTEM IDENTIFICATION FOR THE STANDARD OSWEC WHERE THE INPUT IS TORQUE AND THE OUTPUT IS ANGULAR VELOCITY. RED IS THE NONPARAMETRIC IDENTIFICATION; BLUE IS A SECOND-ORDER SYSTEM ESTIMATE.

that maximizes the power released at that impedance. We can separate the real and imaginary components of both impedances as:

$$Z_w = R_w + I_w \tag{2}$$
$$Z_p = R_p + I_p \tag{3}$$

This is the same setup as the classical maximum power transfer theorem. We will denote the power of the PTO as P_p:

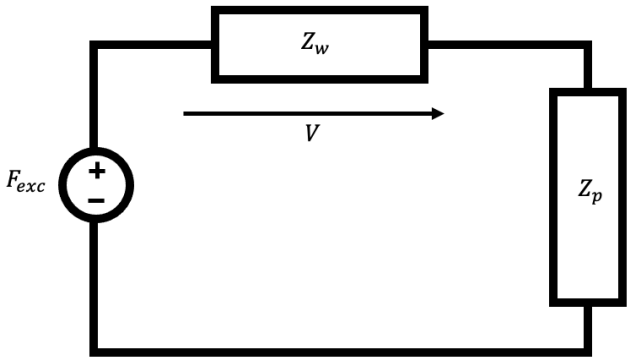

FIGURE 8: ELECTRIC CIRCUIT REPRESENTATION OF WEC DYNAMICS.

$$
\begin{aligned}
|V| &= \frac{|F_{exc}|}{|Z_w + Z_p|} \\
P_p &= V^2 R_w \\
&= \frac{|F_{exc}|^2}{|Z_w + Z_p|^2} R_w \\
&= \frac{|F_{exc}|^2 R_w}{(R_w + R_p)^2 + (I_w + I_p)^2}
\end{aligned}
$$

Solving $\frac{\partial P_p}{R_p} = 0$ and $\frac{\partial P_p}{I_p} = 0$ gives $R_p = R_w$ and $I_p = -I_w$, which is to say that the optimal controller is $Z_p = Z_w^*$, where * denotes the complex conjugate. Z_w was found to be roughly second-order using system identification.

It is important to note that the numerator of these transfer functions is of lower order than the denominator. This means that the optimal controller Z_p is an improper transfer function and cannot be physically realized. However, at a specific frequency, the gain and phase of the optimal controller can be matched using a simple PI controller. This will optimally capture energy at the matched frequency but will be suboptimal at absorbing energy at other frequencies.

These PTOs will be tested using irregular waves, which contain many frequencies; however, a PI controller was still used. The proportional and integral gains were found by grid search for the most mechanical energy in regular waves for 100 s with a 30 s ramp time. The resulting gains from the grid search on regular waves were then used in irregular waves with the same peak period (either 10 or 20 s). Longer simulations would be better but were not done due to the computational time involved in running a grid search. The wave height was 2.5 m. Separate grid searches were performed for each period/PTO combo; that is, one grid search was performed for PI gains for the electric PTO far from resonance, another grid search was conducted for the electric PTO close to resonance, and two more were done for the hydraulic PTO in waves with periods both close to and far from resonance. The grid search for the electric PTO PI gains is shown in Figure 9. The optimal gains from the mechanical energy grid search (Figure 9a) are the gains used. The grid search for electric energy (Figure 9b) is shown only to demonstrate the effect of electric PTO losses. The gains k_p and k_i relate the feedback of velocity (V) to PTO torque (T) as in Equation 4:

$$
\frac{T}{V} = \frac{k_p s + k_i}{s} \tag{4}
$$

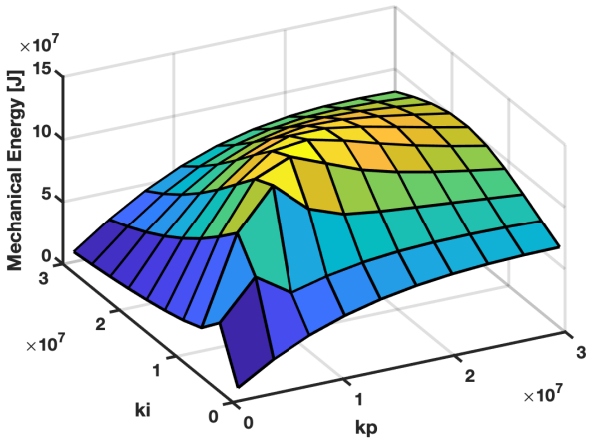

(a) Grid search for mechanical energy

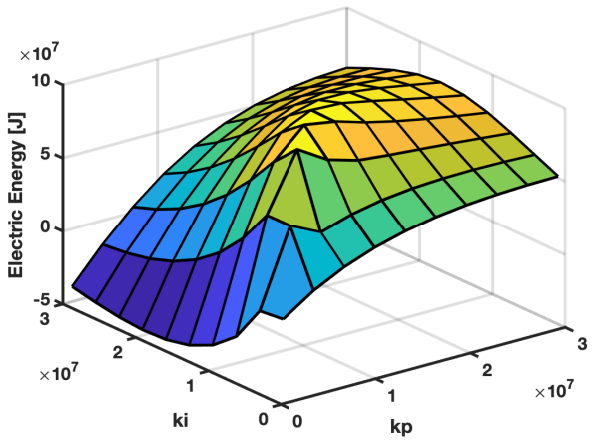

(b) Grid search for electric energy

FIGURE 9: GRID SEARCH FOR PI GAINS FOR THE ELECTRIC PTO IN REGULAR WAVES WITH A 10 S PEAK PERIOD. k_p AND k_i ARE DEFINED IN EQUATION 4.

Note that while this controller uses a proportional term and an integral term (thus the name PI control), it is slightly different than the conventional PI control. Usually, PI control is used to track a reference signal. The input to the PI control is error. Here, however, the input is velocity, and the gains are not set to drive the input to zero, as they are in conventional reference tracking PI control.

The controller for the directly electrified PTO takes velocity as an input and calculates an electric torque. This torque will usually oppose motion; thus, energy will be absorbed by the PTO, but at other times energy will be released, requiring energy from the grid or the battery. In the case of the active valving PTO, the force will be rounded to the nearest possible discrete force

option. None of this control analysis applies to the check valve PTO. CCC is not approximated by this PTO. Instead, a Coulomb damping control is enforced automatically by the check valves.

4. RESULTS

The three PTOs were simulated on the standard OSWEC using WEC-Sim. Because of the lack of information on the sea states of the HAWSEC deployment site, two sets of simulations were done, one with a peak period close to resonance (20 s) and another with a much shorter peak period (10 s). Irregular waves were used with a Pierson-Moskowitz (PM) spectrum of significant wave height, 2.5 m. A 100 s ramp time was included. The simulation lasted 500 s, and a phase seed was used to ensure that each PTO encountered the same waves.

To compare the PTO performance across sea states, we will use the capture width ratio (CWR), which is defined as:

$$\text{CWR} = \frac{P_{absorb}}{Jb}$$

where P_{absorb} is the average absorbed power, J is the average wave energy resource per unit wave crest, and b is the width of the device. Mechanical CWR refers to the absorbed power at the interface between the PTO and the OSWEC. The controllers used in this study seek to maximize mechanical power, not electrical power; thus, the mechanical CWR is a proxy measure of the controllability conferred by the PTO. Electric CWR here refers to where the absorbed power is considered at the electric cables of the generator. The electric CWR is a measure of the overall effectiveness of the PTO.

4.1 Active Valving PTO

The active valving PTO was simulated with both two rails and three rails, and the resulting PTO forces enacted are shown in Figure 10. Two pressure rails results in four force options while the three-rail PTO has nine force options.

If the continuous PI control force was able to be enacted, the CWR would be 1.02 in waves away from resonance. With three pressure rails, the mechanical CWR falls to 1.00 because of the force discretization, and two pressure rails results in a mechanical CWR of 0.87. In waves close to resonance, if the continuous PI control force was able to be enacted, the mechanical CWR would be 0.60. With three pressure rails, the mechanical CWR falls to 0.59, and two pressure rails results in a mechanical CWR of 0.58.

The electric CWR far from resonance is 0.69 for two rails and 0.80 for three rails. Close to resonance the electric CWR is 0.46 for two rails and 0.47 for three rails.

4.2 Check Valve PTO

The check valve PTO is identical to the active valving PTO other than the operation of the valves. The simple control of the check valve PTO brings the mechanical CWR for waves away from resonance to 0.45. For waves close to resonance, the mechanical CWR becomes 0.44. The electric CWR is 0.36 both close to resonance and far from it. The closeness of the CWR values does not mean that the amount of energy absorbed by each is similar; it only means that the proportion of energy absorbed relative to the wave energy resource is similar.

4.3 Direct Electrification

The directly electrified PTO was simulated, and the resulting power is shown in Figure 11. Because there is no power storage element in this PTO, the electric power is sometimes negative, meaning that power is required from the grid or battery. The mechanical CWR is 0.9517 in waves away from resonance, and the electric CWR is 0.6826. The mechanical CWR is 0.4591 in waves close to resonance, and the electric CWR is 0.3297.

4.4 Comparison

The mechanical and electrical CWRs are tabulated in Tables 1 and 2, respectively. Note that the CWRs are larger far from resonance; this does not mean that more energy was captured, but rather that a higher proportion of energy was captured relative to the available wave energy resource.

Mechanical CWR	Far from Resonance	Close to Resonance
Check Valve	0.447	0.444
2 Rail Active Valving	0.866	0.576
3 Rail Active Valving	1.002	0.591
Direct Electrification	0.952	0.459

TABLE 1: MECHANICAL CAPTURE WIDTH RATIO

Electric CWR	Far from Resonance	Close to Resonance
Check Valve	0.358	0.356
2 Rail Active Valving	0.693	0.461
3 Rail Active Valving	0.801	0.473
Direct Electrification	0.683	0.3297

TABLE 2: ELECTRIC CAPTURE WIDTH RATIO

4.5 Scaled Results

The previous results were for the standard WEC-Sim OSWEC model. This device is rectangular, whereas the HAWSEC is roughly square. The standard OSWEC is 9.5 times larger in flap height and 18 times larger in flap width. A scaling factor of 18 is used because oscillating flap WECs are more sensitive to the width dimension than the height [14]. In order to scale calculated quantities down to the smaller scale, Froude scaling is used. Froude scaling scales torque with λ^4 and angular speed with $\lambda^{-0.5}$; thus, power scales with $\lambda^{3.5}$.

The HAWSEC was modeled and simulated in WEC-Sim [3][1]. The system identification technique from Section 3 was repeated on the HAWSEC model, and the frequency response was compared to the Froude scaled frequency response of the standard WEC-Sim OSWEC model. This comparison is shown in Figure 12. Again, the input is torque and the output is angular speed. While the general shape of the frequency response is nearly identical, there are striking differences in both the magnitude and resonant frequency. The phase response estimate from the scaled standard OSWEC is much smoother than than the response estimated from the HAWSEC. This may be because the magnitude response of the HAWSEC is so much smaller, and estimating the phase of such a small oscillation is more difficult.

[1]Design and modeling of the HAWSEC was done at University of Hawai'i by Kyle Pappas, Troy Heitman, Pat Cross, and Krisnakumar Rajagopalan.

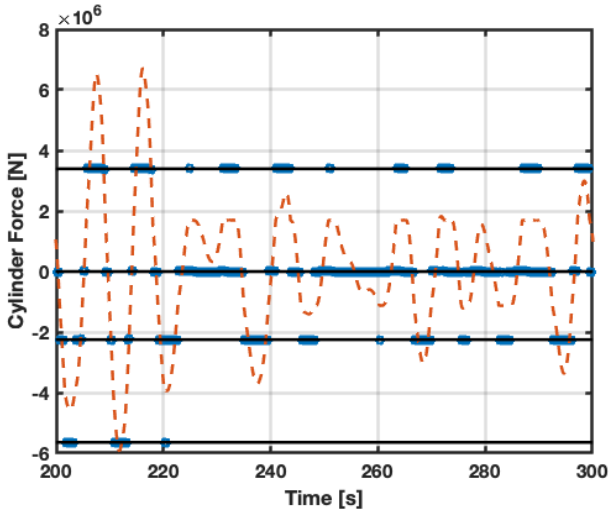

(a) PTO force of active valving PTO with two pressure rails far from resonance

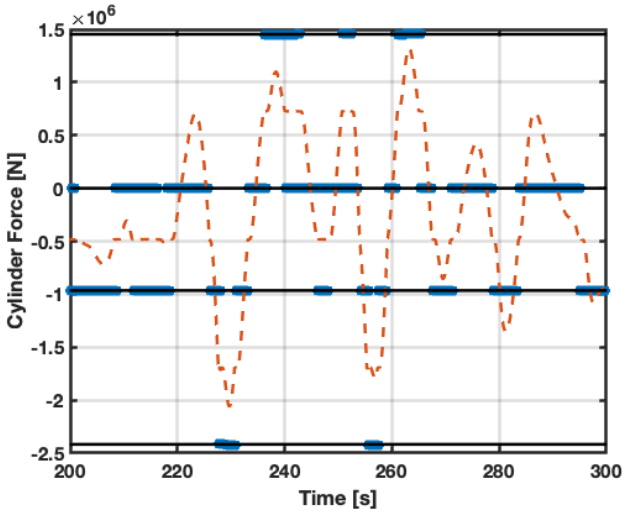

(b) PTO force of active valving PTO with two pressure rails close to resonance

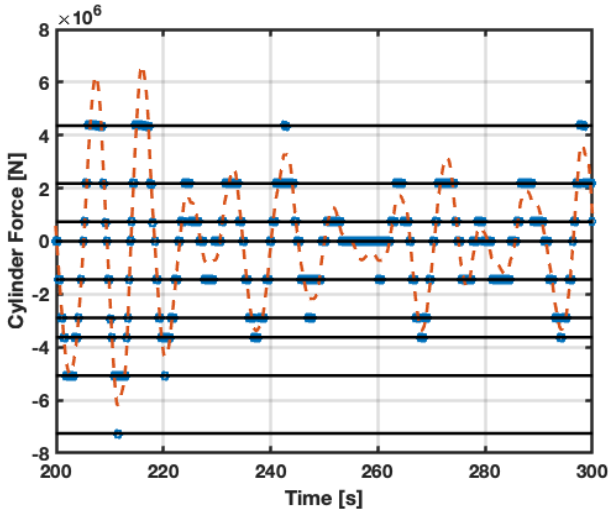

(c) PTO force of active valving PTO with three pressure rails far from resonance

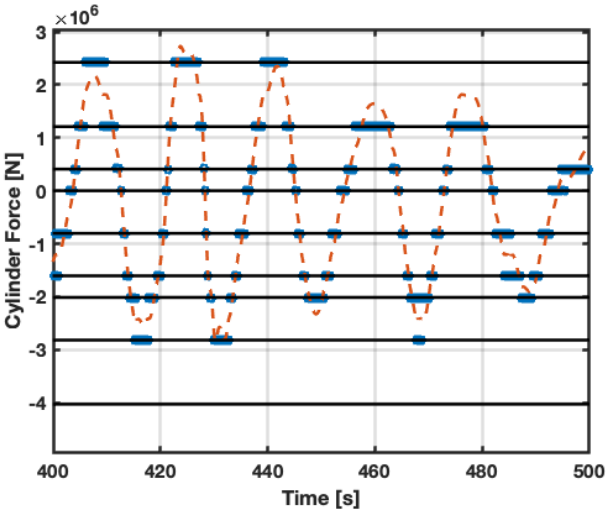

(d) PTO force of active valving PTO with three pressure rails close to resonance

FIGURE 10: PTO FORCE GENERATION IN ACTIVE VALVING PTO. DISCRETE FORCE OPTIONS ARE SHOWN IN BLACK. RED IS THE CONTINUOUS PI CONTROL FORCE. BLUE IS THE ACTUAL FORCE ENACTED BY THE PTO.

A directly electrified PTO was simulated on the HAWSEC, and the results were compared to the scaled standard OSWEC results (see Figure 13). The same wave phase seed was used, and the significant wave height and period were scaled according to Froude scaling. The standard OSWEC was simulated with a significant wave height of 2.5 m and a significant wave period of 10 or 20 s; the HAWSEC was simulated with a $\frac{2.5}{18} = 0.14$ m significant wave height and a $\frac{10}{\sqrt{18}} = 2.4$ s period. Very poor agreement is seen in torque and speed between the scaled standard OSWEC results and the HAWSEC results, but reasonable agreement is seen in power.

5. MODEL LIMITATIONS

This study was intended to be a coarse investigation of PTO options for the HAWSEC. Many simplifications were made knowing that further analysis could be done to improve model fidelity. Still, we attempted to make each PTO benefit roughly equally from the simplifications. A major assumption was that there was no friction in any PTO. Friction will lessen the energy capture of all PTOs but will probably impact the hydraulic PTOs least because they benefit from the lubrication of the hydraulic oil.

The effect of running electric cable or hydraulic hose from the device to shore was not investigated here. This is likely to play a major role in energy capture, but it is unclear whether more losses will result from voltage drop across the electric subsea cable, or from pressure drop and fluid inertia due to the long hydraulic hose.

The pressure rail system of the hydraulic PTOs is simplified significantly. The motor and generator cannot actually remove

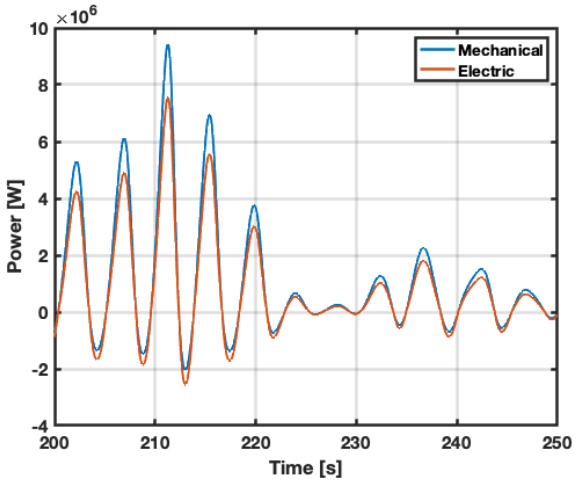

(a) Far from resonance (10 s peak period)

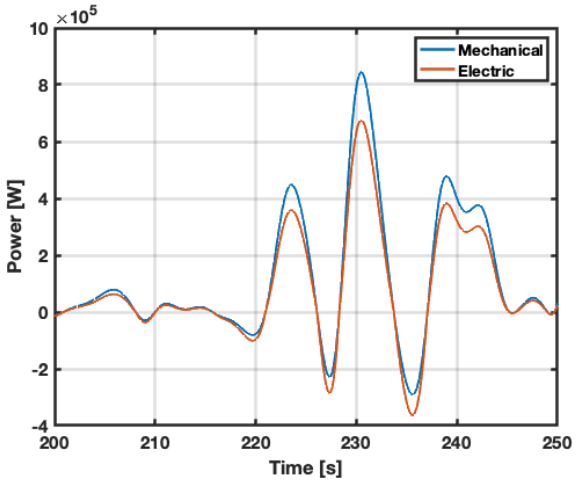

(b) Close to resonance (20 s peak period)

FIGURE 11: POWER PROFILE FOR THE DIRECTLY ELECTRIFIED PTO. BLUE IS THE MECHANICAL POWER AT THE SHAFT CONNECTED TO THE AXIS OF ROTATION OF THE WEC. RED IS THE ELECTRIC POWER THAT WOULD RESULT FROM A CONSTANT COMBINED 80% EFFICIENCY OF THE GENERATOR AND GEARBOX.

average power. They must be at least a little oversized to avoid excessive pressure fluctuations in the accumulators. The pressure rails for both hydraulic systems were chosen very subjectively. A closer study could improve both hydraulic PTOs. Also, the pressure rails could be made to change with sea state. The effect of operating condition on the efficiency of the motor and generator was not included here because these components are expected to operate in a very small operating range due to the nearly constant pressure in the rails.

A major assumption made in this analysis is that the hydraulic PTOs can switch between force options instantaneously. Fluid compressibility and valve dynamics were not studied here but certainly play a major role in the effectiveness of these PTOs.

The standard OSWEC is rectangular, whereas HAWSEC is square. Scaling was done to equate the lengths of the two flaps.

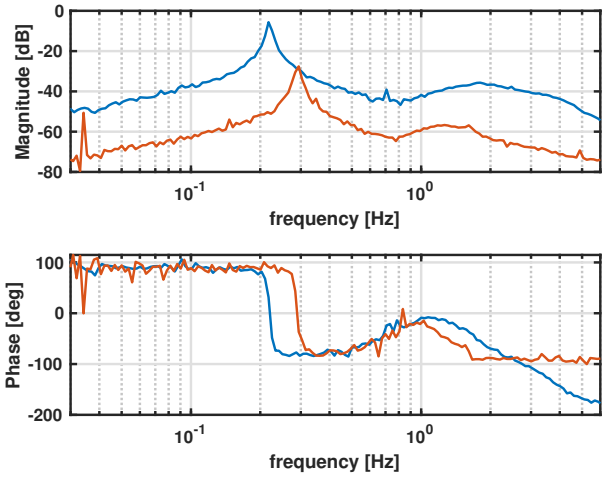

FIGURE 12: COMPARISON BETWEEN THE SCALED STANDARD OSWEC (BLUE) AND THE HAWSEC (RED) FREQUENCY RESPONSES.

The ratio of height to length has been shown to be important but is neglected here [14]. Also, the deployment site of the HAWSEC is very close to shore (<10 m) and might get crashing waves, whereas the standard OSWEC would be further from shore. The effect of crashing waves is not studied here. The water depth was also not scaled by Froude scaling; the default water depth (10.9 m) was used for the standard OSWEC simulations, but the HAWSEC is in 1.06 m water depth. Such discrepancies are believed to be the reason for the poor agreement between the scaled standard OSWEC results and the HAWSEC results.

6. DISCUSSION

Three PTOs were simulated on the standard WEC-Sim OSWEC model and the CWRs were recorded. If the incoming waves have a peak frequency close to the resonant frequency of the device, then the choice of PTO is not consequential with regard to energy capture. This can be seen by the similarity of all the CWRs in the "Close to Resonance" column in Tables 1 and 2. However, if energy is present at frequencies far from device resonance, the control system of the PTO gives a significant advantage with respect to energy capture. The active valving and direct electrification PTOs have a definite advantage on the check valve PTO when incoming waves are far from the resonant period.

Of all the PTOs studied here, the three-rail active valving PTO showed the largest CWR ratio, both mechanical and electrical, close to resonance and far from it. However, this is by far the most complicated PTO, and a scheme for removing flow from each pressure rail using only one motor has not yet been developed, although it is possible. Simpler designs, like the two-rail active valving and the direct electrification PTOs are preferred due to the reduction of failure modes and improved durability.

An important consideration for small-scale WECs is the availability of off-the-shelf components that are compatible with the marine environment. Hydraulic PTOs have an advantage in this regard because hydraulic cylinders are already used in many

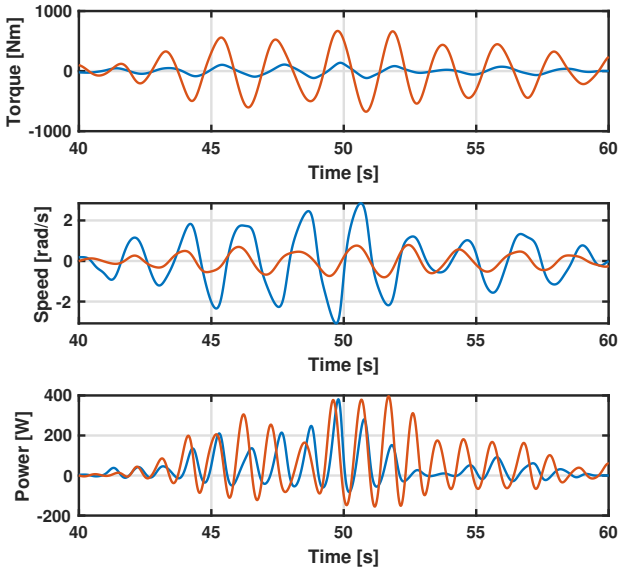

FIGURE 13: COMPARISON BETWEEN THE SCALED STANDARD OSWEC RESULTS (BLUE) AND THE HAWSEC RESULTS (RED) USING A DIRECTLY ELECTRIFIED PTO. THE POWER SHOWN IS MECHANICAL POWER.

marine applications and are commercially available. Conversely, generators that are designed for marine applications are extremely difficult to source, and custom building can be expensive. The HAWSEC is planned to be deployed very close to a pier, from which a hydraulic hose can run. This allows motors, accumulators, valves, and generators to be operated in a safe, non-harsh environment, either on shore or on the pier. Future work will include analysis of the effect of long amounts of hydraulic hosing [15].

The electric PTO is a potentially good choice for this application because of the low power and torque requirements of the HAWSEC. In large-scale WECs, downsizing the peak power requirement of the electric generators is important for PTO cost. However, at a small scale, the power is already so small that downsizing the electric motor does not have a substantial effect. Also, because torque decreases so dramatically with WEC size, much less gearing is required for small-scale WECs than for large-scale WECs. However, as this is a small-scale project, it is not economically feasible to custom-build the PTO components. Off-the-shelf submersible generators and gearboxes are not readily commercially available. Designing and building submersible generators is feasible for large projects that require custom components regardless of PTO architecture, but is less feasible for small-scale projects that can rely on off-the-shelf components.

Primarily for this reason, the directly electrified PTO is not chosen for use on the HAWSEC; rather, a two-pressure-rail active valving hydraulic PTO that can utilize off-the-shelf components is selected. Between the hydraulic PTOs analyzed here, the two-rail active valving PTO is selected over the check valve PTO because of the improved controllability, increased power capture, and only marginally higher equal cost (solenoid valves are slightly more expensive than check valves).

This conclusion was made using results from the large-scale standard WEC-Sim OSWEC model. But when the scaled standard OSWEC results were compared to the HAWSEC, clear and striking differences were seen. The HAWSEC had much larger torque and much smaller angular speed than was predicted by the standard OSWEC model. Further work is required to investigate why the scaled results disagree so much with the small-scale model. It believed that the main problem is improper and imprecise scaling of the two models. The shape of the OSWEC is different, which was not accounted for here. Also, the water depth was not scaled according to Froude scaling. Proper scaling was not done because the small-scale model was initially unavailable, so there was no way to scale up the model carefully. Once the small model was available, it was more accurate to just use the small model to make design decisions, so there was no longer a need for scaling. The cautious conclusion (further work is needed) of this scaling comparison is that care must be taken when scaling models (at least OSWEC models). Simply selecting a WEC model that seems similar to the small-scale design may not yield even order of magnitude accuracy.

7. ACKNOWLEDGEMENTS

This work was authored in part by the National Renewable Energy Laboratory, operated by Alliance for Sustainable Energy, LLC, for the U.S. Department of Energy (DOE) under Contract No. DE-AC36-08GO28308. Funding provided by U.S. Department of Energy Office of Energy Efficiency and Renewable Energy Water Power Technologies Office . The views expressed in the article do not necessarily represent the views of the DOE or the U.S. Government. The U.S. Government retains and the publisher, by accepting the article for publication, acknowledges that the U.S. Government retains a nonexclusive, paid-up, irrevocable, worldwide license to publish or reproduce the published form of this work, or allow others to do so, for U.S. Government purposes.

REFERENCES

[1] Zurkinden, Andrew Stephen, Lambertsen, Søren Heide, Damkilde, Lars, Gao, Zhen and Moan, Torgeir. "Fatigue analysis of a point absorber wave energy converter subjected to passive and reactive control." *Journal of Offshore Mechanics and Arctic Engineering* Vol. 137 No. 5 (2015).

[2] Yu, Yi-Hsiang, Tom, Nathan and Jenne, Dale. "Numerical analysis on hydraulic power take-off for wave energy converter and power smoothing methods." *International Conference on Offshore Mechanics and Arctic Engineering*, Vol. 51319: p. V010T09A043. 2018. American Society of Mechanical Engineers.

[3] Husain, Kelley Ruehl David Ogden Yi-Hsiang Yu Adam Keester Nathan Tom Dominic Forbush Jorge Leon Jeff Grasberger Salman. "WEC-Sim v5.0.1." (2022). DOI 10.5281/zenodo.7121186. URL https://zenodo.org/badge/latestdoi/20451353.

[4] Penalba, Markel, Sell, Nathan, Hillis, Andy and Ringwood, John. "Validating a wave-to-wire model for a wave

energy converterpart I: The Hydraulic Transmission System." *Energies* Vol. 10 No. 7 (2017): p. 977. DOI 10.3390/en10070977.

[5] Yu, Y. H., Jenne, D. S., Thresher, R., Copping, A., Geerlofs, S. and Hanna, L. A. "Reference model 5 (RM5): Oscillating Surge Wave Energy converter." (2015)DOI 10.2172/1169778.

[6] Cargo, CJ, Hillis, AJ and Plummer, AR. "Optimisation and control of a hydraulic power take-off unit for a wave energy converter in irregular waves." *Proceedings of the Institution of Mechanical Engineers, Part A: Journal of Power and Energy* Vol. 228 No. 4 (2014): pp. 462–479.

[7] Wills, Jackson, Keester, Adam and Li, Perry Y. "A Power Take-Off (PTO) for Wave Energy Converters Based on the Hybrid Hydraulic-Electric Architecture (HHEA)." *Fluid Power Systems Technology*, Vol. 85239: p. V001T01A039. 2021. American Society of Mechanical Engineers.

[8] Hansen, Rico H, Kramer, Morten M and Vidal, Enrique. "Discrete displacement hydraulic power take-off system for the wavestar wave energy converter." *Energies* Vol. 6 No. 8 (2013): pp. 4001–4044.

[9] Henderson, Ross. "Design, simulation, and testing of a novel hydraulic power take-off system for the Pelamis wave energy converter." *Renewable energy* Vol. 31 No. 2 (2006): pp. 271–283.

[10] OSullivan, Dara, Griffiths, James, Egan, Michael G and Lewis, Anthony W. "Development of an electrical power take off system for a sea-test scaled offshore wave energy device." *Renewable Energy* Vol. 36 No. 4 (2011): pp. 1236–1244.

[11] Coe, Ryan Geoffrey, Bacelli, Giorgio, Forbush, Dominic, Spencer, Steven James, Dullea, Kevin J, Bosma, Bret and Lomonaco, Pedro. "FOSWEC dynamics and controls test report." Technical report no. Sandia National Lab.(SNL-NM), Albuquerque, NM (United States). 2020.

[12] Papoulis, Athanasios and Unnikrishna Pillai, S. *Probability, random variables and stochastic processes* (2002).

[13] Falnes, Johannes and Kurniawan, Adi. *Ocean waves and oscillating systems: linear interactions including wave-energy extraction*. Vol. 8. Cambridge university press (2020).

[14] Gomes, RPF, Lopes, MFP, Henriques, JCC, Gato, LMC and Falcão, AFO. "The dynamics and power extraction of bottom-hinged plate wave energy converters in regular and irregular waves." *Ocean Engineering* Vol. 96 (2015): pp. 86–99.

[15] Simmons, Jeremy W and Van de Ven, James D. "Pipeline Model Fidelity for Wave Energy System Models." *Fluid Power Systems Technology*, Vol. 85239: p. V001T01A011. 2021. American Society of Mechanical Engineers.